

# Stringy signals from large-angle correlations in the cosmic microwave background?

Miguel-Angel Sanchis-Lozano\*

*Instituto de Física Corpuscular (IFIC) and Departamento de Física Teórica  
CSIC-University of Valencia, Dr. Moliner 50, E-46100 Burjassot, Spain*

## Abstract

We interpret the lack of large-angle temperature correlations and the apparent even-odd parity imbalance, observed in the cosmic microwave background by COBE, WMAP and *Planck* satellite missions, as a possible stringy signal ultimately stemming from a composite inflaton field (e.g. a fermionic condensate). Based on causality arguments and a Fourier analysis of the angular two-point correlation function, *two* infrared cutoffs  $k_{\min}^{\text{even,odd}}$  are introduced in the CMB power spectrum associated, respectively, with periodic and antiperiodic boundary conditions of the fermionic constituents (echoing the Neveu-Schwarz-Ramond model in superstring theory), without resorting to any particular model.

\*E-mail address: Miguel.Angel.Sanchis@ific.uv.es

# 1 Introduction

Since its discovery in 1964 by Penzias and Wilson, the study of the cosmic microwave background (CMB) has provided a wealth of information on the early universe and its evolution, even going back in time closer to the Big Bang than the recombination phase when it was released. Indeed, to explain the outstanding homogeneity of the CMB temperature across the sky, an inflationary phase has been put forward to solve the so-called horizon problem, together with the flatness issue and “unwanted” relics, like unseen magnetic monopoles [1].

Although there are alternative models (see e.g. [2], [3]), inflation has currently become the commonly accepted paradigm to explain cosmological evolution because of a series of convincing reasons of which we just highlight one: observations of the CMB temperatures across the sky show that the universe is approximately uniform and homogeneous at scales much larger than the particle horizon at decoupling time, and a phase of exponential growth can account for this.

In principle, all what is needed for a successful inflation is a scalar field satisfying the slow-roll conditions and a graceful exit. Actually the inflaton needs not be a fundamental (nor single) scalar field but an effective, e.g. composite, field (see Ref. [4] for a review) stemming from more fundamental interacting fields (like a fermionic condensate<sup>1</sup>). Through the process of inflation, initial small quantum fluctuations of the underlying inflationary field when exiting the Hubble horizon would have formed the seeds for the matter distribution and subsequent growth to structures seen in today’s universe, showing an overall isotropy and homogeneity at large scales. Alternatively, in a linearly expanding cosmology, like the so-called  $R_h = ct$  universe (for an exhaustive review of this model see [8]), the quantum fluctuations of the primordial field driving the expansion turned into (semi-)classical fluctuations once exiting the Planck domain at about the Planck time [9].

On the other hand, in spite of the many successes of the Standard Cosmological Model ( $\Lambda$ CDM), anomalies and tensions have emerged from a variety of astrophysical and cosmological observations (see e.g. [10], [2], [11]). In particular, the observed but unexpected lack of large-angle angular correlations (related to the missing power at low multipoles), together with the odd-parity dominance in the two-point correlation function of the CMB were examined in detail in Ref. [12]. To this end, an infrared cutoff was set in the primordial CMB power spectrum following the original work of [13]. At the same time, odd-parity dominance was taken into account by weighting the different multipole contributions to angular correlations. Needless to say, such a parity imbalance questions the large-scale isotropy of the observable universe and hence the Cosmological Principle.

Here we shall perform a similar analysis but introducing two infrared cutoffs to the CMB power spectrum ( $k_{\min}^{\text{even}}, k_{\min}^{\text{odd}}$ ), affecting differently even- and odd-parity multipole contributions in the best fit of the two-point correlation function  $C(\theta)$ . Firstly, the aim of using two infrared cutoffs, rather than one, is to simultaneously achieve both goals (reproducing missing large-angle correlations and odd-parity dominance) with fewer fitting parameters, while suggesting an interesting and novel physical interpretation. Indeed, large-angle correlations should provide details on the very first stages of the universe maybe hinting new physics at unexplored large scales. This possibility stands as the main motivation of this paper.

In order to get the best fit of  $C(\theta)$  to *Planck* 2018 data, we find that the ratio  $k_{\min}^{\text{even}}/k_{\min}^{\text{odd}}$  should be numerically close to 2. Later, we will provide a tentative theoretical explanation for this, based on an assumed “stringy”<sup>2</sup> behaviour of the fundamental (fermionic) field(s) driving inflation in the early universe.

---

<sup>1</sup>Historically, the interpretation of scalars as fermionic bound states, e.g. in the Nambu-Jona-Lasinio model, dates back to the sixties in the past century, to address strong interaction issues [5], [6]). The possibility of a composite Higgs boson is also contemplated [7].

<sup>2</sup>In this paper *stringy* refers generically to properties associated with periodic and antiperiodic boundary conditions like those found in superstring theory [14], and not, in principle, to cosmic strings understood as one-dimensional structures of false vacuum [1].

## 2 Analysis of angular correlations in the CMB

All three COBE, WMAP and *Planck* satellite missions have observed that the temperature angular distribution of the CMB is remarkably homogeneous across the sky, with anisotropies of order 1 part in  $10^5$ . A powerful test of these fluctuations relies on the two-point (and higher) angular correlation function  $C(\theta)$ , defined as the ensemble product of the temperature differences with respect to the average temperature, from all pairs of directions in the sky defined by unitary vectors  $\vec{n}_1$  and  $\vec{n}_2$ :

$$C(\theta) = \left\langle \frac{\delta T(\vec{n}_1)}{T} \frac{\delta T(\vec{n}_2)}{T} \right\rangle, \quad (1)$$

where  $\theta \in [0, \pi]$  is the angle defined by the scalar product  $\vec{n}_1 \cdot \vec{n}_2$ .

Assuming azimuthal symmetry,  $C(\theta)$  can be expanded using the Legendre polynomials as:

$$C(\theta) = \frac{1}{4\pi} \sum_{\ell=2}^{\infty} (2\ell + 1) C_{\ell} P_{\ell}(\cos(\theta)), \quad (2)$$

where the  $C_{\ell}$  multipole coefficients encode the information with astrophysical/cosmological significance. In practice, the sum starts at  $\ell = 2$  and ends at a given  $\ell_{\max}$ , dictated by the resolution of the data (in our case we set  $\ell = 400$  as an upper limit). The first two terms are excluded because (i) the monopole ( $\ell = 0$ ) is simply the average temperature over the whole sky and plays no role in the correlations, other than a global scale shift; and (ii) the dipole ( $\ell = 1$ ) is greatly affected by Earth's motion, creating an anisotropy dominating over the intrinsic cosmological dipole signal, being usually removed from the multipole analysis.

Under some simplifying assumptions [15], the coefficients  $C_{\ell}$  in Eq.(2) can be evaluated according to the following expression

$$C_{\ell} = N \int_0^{\infty} dk k^{n_s-1} j_{\ell}^2(kr_d), \quad (3)$$

where  $N$  is a normalization constant,  $n_s \approx 1$  is the spectral index and  $j_{\ell}(kr_d)$  denotes the spherical Bessel function of order  $\ell$ , whose argument involves the comoving distance  $r_d$  from the last scattering surface (LSS) to us, and the wavenumber  $k$  for each mode in the CMB power spectrum which varies, in principle, from zero to infinity [15].

### 2.1 Single infrared cutoff in the CMB power spectrum

As already commented, large-angle temperature correlations in the CMB provide information on the earliest stages of the primitive Universe, well before recombination and the subsequent formation of the cosmic structure [15]. In this regard, the  $C(\theta)$  function defined in Eq.(2) was found close to zero above  $60^{\circ} - 70^{\circ}$  from all three COBE, WMAP and *Planck* data, constituting one of the anomalies between standard cosmology and observations [10]. Indeed, the suppression of large-angle correlations together with the existence of a downward tail at large angles ( $\gtrsim 150^{\circ}$ ) were unexpected in standard cosmology, given that inflation is supposed to provide the required number of e-folds ( $\gtrsim 60$ ) to solve both the horizon and flatness problems, thereby bringing angular coverage across the full sky.

In order to mitigate this tension, the authors of [13] introduced an infrared cutoff in the CMB power spectrum, leading to a lower limit  $k_{\min}$  in the integral:

$$C_{\ell} = N \int_{k_{\min}}^{\infty} dk k^{n_s-1} j_{\ell}^2(kr_d). \quad (4)$$

The normalization constant  $N$  and  $k_{\min}$  are obtained from a global fit to the whole angular correlation function.

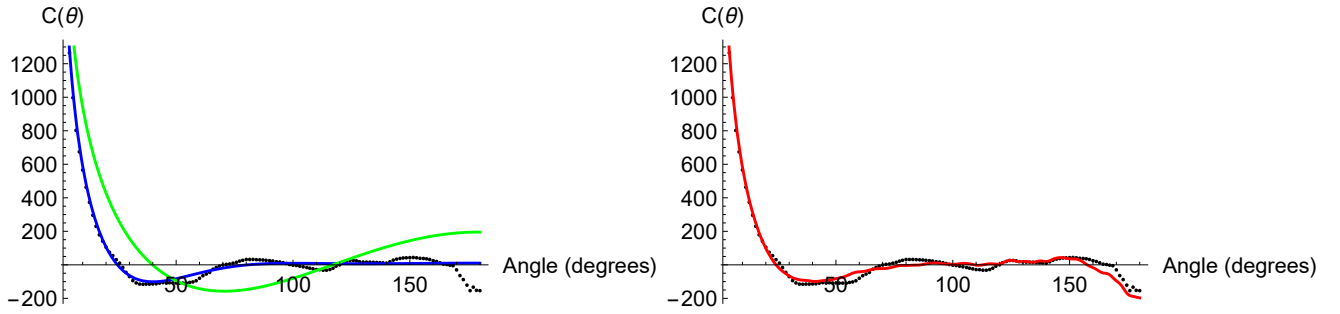


Figure 1: Two-point correlation function  $C(\theta)$  (solid curves) obtained from the fit to *Planck* 2018 data (a) Left panel:  $\Lambda$ CDM prediction (in green) clearly deviating from data in almost the whole angular range; blue curve:  $u_{\min} = 4.5$  without imposing odd-dominance requirement. (b) Right panel: Red curve for  $u_{\min}^{\text{even}} = 4.5$  with odd-parity dominance from [12].

A theoretical motivation to this truncation of  $k$  modes entering the integral of Eq.(4), relies on the existence of a maximum correlation length obtained from a causality requirement at decoupling time  $t_d$  [16], [13]:

$$\lambda_{\max} = 2\pi R_h, \quad (5)$$

where  $R_h$  stands for the Hubble radius at that time. Actually the Hubble radius  $R_h$  not necessarily is a true horizon, but should provide an order of magnitude estimate of the maximum correlation length. In fact  $\lambda_{\max} = \alpha 2\pi R_h$ , where  $\alpha \leq 1$  depends on the cosmological model, e.g.  $\alpha \approx 0.5$  for the  $\Lambda$ CDM [18].

On the other hand, the comoving wavenumber  $k_{\min}$  associated with  $\lambda_{\max}$  reads

$$k_{\min} = \frac{2\pi a(t)}{\lambda_{\max}}, \quad (6)$$

which can be interpreted as the first quantum fluctuation in the underlying primordial field driving the early universe expansion either (i) having crossed the Hubble horizon once inflation started, or (ii) having emerged out of the Planck domain [9] should inflation have never happened, as in a  $R_h = ct$  universe [8].

Next, changing the integration variable in Equation (3) from  $k$  to the dimensionless variable  $u \equiv kr_d$  and setting  $n_s = 1$  for simplicity, one gets

$$C_\ell = N \int_{u_{\min}}^{\infty} du \frac{j_\ell^2(u)}{u}. \quad (7)$$

Let us point out that only those  $C_\ell$  coefficients with  $\ell \lesssim 10$  are actually affected by the lower cutoff  $u_{\min} = k_{\min}r_d \neq 0$  in the above integral.

In Ref. [12] the numerical interval  $u_{\min} = 4.5 \pm 0.5$  was obtained from a best fit to the *Planck* 2018 dataset [17]. In the left panel of Figure 1 we plot  $C(\theta)$  corresponding to the  $\Lambda$ CDM prediction ( $u_{\min} = 0$ ), together with the best fit to the same *Planck* data as done in [13] with  $u_{\min} = 4.5$  without breaking even-odd parity balance. One can see at once that standard cosmology fails to fit the data, while the latter curve indeed yields almost zero correlations above  $\simeq 70^\circ$ , but fails to reproduce the observed downward tail at  $\sim 180^\circ$ . Finally, in the right panel of Figure 1 we reproduce the excellent fit ( $\chi^2/\text{d.o.f.} \approx 1$ ) done in [12] to the same dataset requiring odd-parity dominance.

On the other hand, the maximum correlation angle  $\theta_{\max}$  can be roughly estimated as

$$\theta_{\max} \simeq \frac{\lambda_{\max}}{R_d} \rightarrow \theta_{\max} \simeq \frac{2\pi}{u_{\min}}, \quad (8)$$

where  $R_d = a(t_d)r_d$  stands for the proper distance from the LSS to us, and  $u_{\min} = k_{\min}r_d$ .

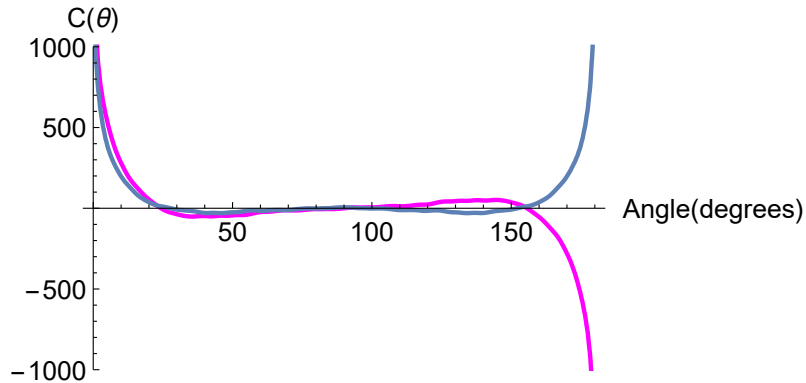


Figure 2: The  $C_{\text{even}}(\theta)$  (in blue) and  $C_{\text{odd}}(\theta)$  (in magenta) contributions to  $C(\theta)$  in Eq. (9), setting  $u_{\text{min}} = 4.5$ . Notice the delicate balance between odd and even  $\ell$ -multipoles (even at high- $\ell$ ) in order to yield zero correlations above  $\approx 60^\circ - 70^\circ$ . Any slight deviation from this balance would yield a downwards (upwards) tail at  $\simeq 180^\circ$  for odd (even) dominance of Legendre polynomials.

For later use, let us regroup the even and odd  $\ell$ -multipoles in Eq.(2), namely

$$C(\theta) = C_{\text{even}}(\theta) + C_{\text{odd}}(\theta) = \frac{1}{4\pi} \sum_{\ell_{\text{even}}} (2\ell + 1) C_\ell P_\ell(\cos(\theta)) + \frac{1}{4\pi} \sum_{\ell_{\text{odd}}} (2\ell + 1) C_\ell P_\ell(\cos(\theta)) \quad (9)$$

To better understand the behaviour of the  $C(\theta)$  curve, we plot in Figure 2 separately the above even and odd parity pieces ( $C_{\text{even}}(\theta)$  and  $C_{\text{odd}}(\theta)$ ), as a function of  $\theta$  for  $\ell \in [2, 400]$ . Because of the oscillatory behaviour of the Legendre polynomials, both contributions add positively at small and middle angles, while a delicate balance is needed in order to get zero correlation at larger angles. This balance is indeed achieved [12] when using a single cutoff  $k_{\text{min}}$  in the evaluation of the  $C_\ell$  coefficients in Eq.(7).

However, if *two* distinct infrared cutoffs apply differently to even and odd  $\ell$ -modes, such a delicate balance will be likely broken. Then odd or even parity dominance can be obtained *naturally*. In the next section we examine in depth this issue of paramount importance in this work.

## 2.2 Two infrared cutoffs in the CMB power spectrum

In Ref. [12], the fit to *Planck* 2018 data was optimized using a  $k_{\text{min}}$  together with the requirement of parity imbalance by weighting adequately the odd and even terms in Eq.(2). We shall now carry out a similar analysis but introducing two infrared cutoffs (rather than one) in the CMB power spectrum, namely,  $k_{\text{min}}^{\text{even}}$  and  $k_{\text{min}}^{\text{odd}}$ , affecting differently the even- and odd-parity coefficients.

The goals of this new analysis are to provide: (i) a common explanation of both missing large-angle correlations and odd-parity dominance with fewer fitting parameters; and (ii) a physical interpretation behind. First, the numerical values of  $k_{\text{min}}^{\text{even}}$  and  $k_{\text{min}}^{\text{odd}}$  were heuristically determined from a fit of  $C(\theta)$  to data, checking its consistency with odd-dominance by means of a parity statistic to be discussed in section 3.1. Depending on which,  $k_{\text{min}}^{\text{even}}$  or  $k_{\text{min}}^{\text{odd}}$  is larger, odd or even dominance can be achieved.

On the one hand, the introduction of two infrared cutoffs in the angular power spectrum can be merely seen as a phenomenological approach to jointly account for missing large-angle correlations and the downwards tail in the  $C(\theta)$  curve. Seen in this way, just one additional fitting parameter is required with respect to the analysis of [13]. On the other hand, however, we claim in this work that the ratio of both infrared cutoffs becomes “fixed by theory”, as a consequence of an extra (fermionic) spin degree of freedom due to the assumed fermionic nature of the underlying inflating field(s). Hence no additional parameter is actually introduced in the fits.

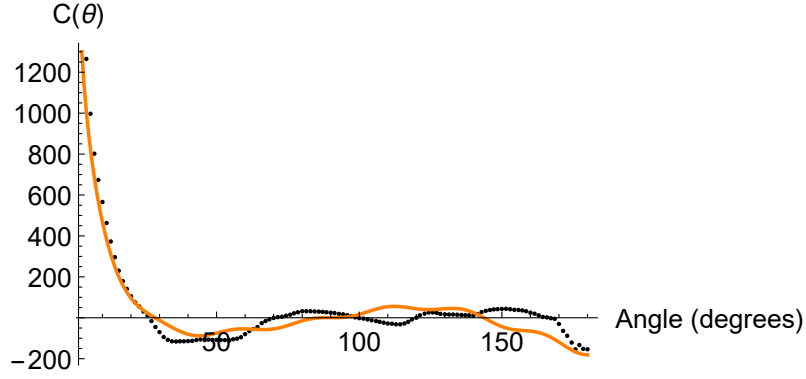


Figure 3: Two-point correlation function  $C(\theta)$  (orange solid curve) obtained from the fit to *Planck* 2018 data for  $u_{\min}^{\text{even}} = 5.34$  and  $u_{\min}^{\text{odd}} = u_{\min}^{\text{even}}/2 = 2.67$ . The fit is not so good as in the right panel of Figure 1, but the number of fitting parameters is quite smaller and, above all, provides a theoretical foundation that explains simultaneously the lack of large-angle correlations and the observed odd-parity dominance leading to a downward tail near  $180^\circ$ .

Therefore we compute separately the  $C_\ell$  coefficients of the even and odd  $\ell$ -multipoles according to

$$C_{\ell_{\text{even/odd}}} = N \int_{u_{\min}^{\text{even/odd}}}^{\infty} du \frac{j_\ell^2(u)}{u}, \quad (10)$$

equivalent to Eq.(7) for a single  $k_{\min}$  without a distinction of parity. Now the integral lower limits are:  $u_{\min}^{\text{even,odd}} = k_{\min}^{\text{even,odd}} r_d$ , respectively, where  $r_d$  denotes again the distance from the LSS to us.

In Figure 3 we plot the fit of  $C(\theta)$  to *Planck* 2018 data under the assumption of two different lower cutoffs  $u_{\min}^{\text{even,odd}}$  in the integral of Eq.(10). Admittedly, the new fit looks a bit worse than in the right panel of Figure 1. However notice that the number of free parameters now is smaller and, above all, one can simultaneously accommodate the lack of large-angle correlations and the apparent odd-dominance showing up as a downward tail at  $\gtrsim 150^\circ$ , without resorting to any further fine-tuning of the  $C_\ell$  coefficients.

Furthermore, a suggestive interpretation emerges as the ratio  $k_{\min}^{\text{even}}$  to  $k_{\min}^{\text{odd}}$  turns out to be numerically near 2. Had we tried the opposite situation  $k_{\min}^{\text{even}} < k_{\min}^{\text{odd}}$ , the  $C(\theta)$  curve would have shown an upward tail, contrary to observational data. The mathematical reason why the condition  $k_{\min}^{\text{even}} > k_{\min}^{\text{odd}}$  goes in the “right” direction is that the  $C_\ell$  coefficients (for  $\ell \lesssim 10$ ) decrease for  $\ell_{\text{odd}}$  to a lower extent than for  $\ell_{\text{even}}$  (as compared to no lower cutoff at all), thereby favoring odd-parity dominance, in accordance with observations.

Next, notice the following relations between Legendre polynomials and the square of cosine functions with entire and half-entire ( $2\pi$ ) periods (these relations can also be formulated in terms of Chebyshev polynomials [22]), called to play a fundamental role in our later development:

$$\begin{aligned} P_1(\cos \theta) &= -1 + 2 \cos^2(\theta/2) \\ P_2(\cos \theta) &= -0.5 + 1.5 \cos^2(\theta) \\ P_3(\cos \theta) &= -1 + 0.75 \cos^2(\theta/2) + 1.25 \cos^2(3\theta/2) \\ P_4(\cos \theta) &= -0.7184 + 0.6249 \cos^2(\theta) + 1.0937 \cos^2(2\theta) \\ P_5(\cos \theta) &= -1 + 0.4687 \cos^2(\theta/2) + 0.5469 \cos^2(3\theta/2) + 0.9844 \cos^2(5\theta/2); \text{ etc} \end{aligned} \quad (11)$$

Higher order Legendre polynomials replicate the same pattern: besides a constant, even and odd polynomials either contain  $\cos^2[n\theta]$  or  $\cos^2[(n+1/2)\theta]$  terms, respectively. Note that this pattern is just mathematical for the moment, but below will be put in correspondence with the Fourier expansion of inflaton field constituents, using a one-dimensional toy-model.

Next, inspired on very general grounds by superstring theory (and obviously without entering at all in its complexity and intricacies [14]), and invoking a similar causality argument as employed for the single  $k_{\min}$  case, we address now the possibility that any constituent (fermionic) field  $\psi(\varphi)$  (for simplicity no more variables or indices are explicitly written) of a composite inflaton <sup>3</sup> satisfies either the periodic or antiperiodic boundary condition:

$$\psi(\varphi + 2\pi) = \psi(\varphi) \tag{12}$$

$$\psi(\varphi + 2\pi) = -\psi(\varphi) \rightarrow \psi(\varphi + 4\pi) = \psi(\varphi) \tag{13}$$

The angular Fourier expansion of  $\psi(\varphi)$  for the periodic condition reads:

$$\psi(\varphi) = \sum_{n \in \mathcal{Z}} \alpha_n e^{in\varphi} \tag{14}$$

and for a real function

$$\psi(\varphi) = 2 \sum_{n \in \mathcal{Z}^+} \text{Re } \alpha_n e^{in\varphi}, \tag{15}$$

so that only  $\cos(n\varphi)$  terms appear in the Fourier expansion.

Let us define now a correlation function as in [24]

$$\int_0^{2\pi} \psi(\varphi) \psi(\varphi + \Delta\varphi) \frac{d\varphi}{2\pi}. \tag{16}$$

For random Gaussian Fourier coefficients, if we define  $\theta = \Delta\varphi/2$  one finds

$$C(\Delta\varphi) = 2 \sum_{n \in \mathcal{Z}^+} C_n \cos(n\Delta\varphi) \rightarrow C(\theta) = 4 \sum_{n \in \mathcal{Z}^+} C_n \cos^2(n\theta) - 2, \tag{17}$$

with  $C_n = \langle \alpha_n \alpha_n^* \rangle$  and  $\theta \in [0, \pi]$  to be identified with the angle appearing as the argument of the two-point correlation function  $C(\theta)$ .

For the antiperiodic conditions, the Fourier expansion reads

$$\psi(\varphi) = \sum_{n \in \mathcal{Z}^+ + 1/2} \alpha_n e^{in\varphi}, \tag{18}$$

which guarantees that it changes sign when  $\varphi \rightarrow \varphi + 2\pi$ . Therefore

$$C(\theta) = 4 \sum_{n \in \mathcal{Z}^+ + 1/2} C_n \cos^2(n\theta) - 2. \tag{19}$$

The above results obtained from this toy-model suggest the assignment of even- and odd-parity  $C_{\text{even}}(\theta)$  and  $C_{\text{odd}}(\theta)$  pieces in Eq.(9), to the periodicity and antiperiodicity conditions given in Eqs.(14-18), respectively, somewhat recalling the well-known Ramond and Neveu-Schwarz sectors in superstring theory [14]. Hereafter we shall assume that the above conclusions apply to the fundamental field(s) driving the expansion of the early universe.

---

<sup>3</sup>The possibility that a fermionic field, minimally or non-minimally coupled with the gravitational field, drives the inflation, without resorting to a composite inflaton, has also been studied (see [23] and references therein).

### 3 Physical interpretation

In the following we will consider, without entering into details, the inflaton as an effective scalar field  $\Phi$  made out of two constituent fermionic fields ( $\Phi = \bar{\Psi}\Psi$ ) driving the expansion of the early universe. The causality condition yielding  $\lambda_{\max}$  used for a single infrared cutoff, is assumed now to split into two conditions applied independently to the periodic and the antiperiodic conditions in virtue of the spin degrees of freedom of the constituent fermionic fields of the effective inflaton.

Hence, in analogy to Eq.(5), we shall now consider two maximum correlation lengths for even and odd parity multipoles, denoted as  $\lambda_{\max}^{\text{even}}$  and  $\lambda_{\max}^{\text{odd}}$ , satisfying

$$\lambda_{\max}^{\text{even}} = 2\pi R_h, \quad \lambda_{\max}^{\text{odd}} = 4\pi R_h. \quad (20)$$

Then two comoving wavenumbers  $k_{\max}^{\text{even}}$  and  $k_{\max}^{\text{odd}}$  can be defined from those length scales:

$$k_{\min}^{\text{odd}} = 2\pi a(t_d)/\lambda_{\max}^{\text{odd}}, \quad k_{\min}^{\text{even}} = 2\pi a(t_d)/\lambda_{\max}^{\text{even}}, \quad (21)$$

corresponding to odd and even parity modes, respectively;  $a(t_d)$  denotes the scale factor at decoupling time. Let us remark that physical momenta are given by  $k/a(t)$ , but the ratio  $k_{\min}^{\text{even}}/k_{\min}^{\text{odd}}$  remains frozen after exiting the horizon. Note also that the numerical values of the lower cutoffs are obtained from a fit to correlation data, and not from Eq.(20). Indeed what really matters in this work is that their ratio is equal (or close) to 2.

On the other hand, two relevant angles can be defined following Eq.(8) for a single  $k_{\min}$ :

$$\theta_{\text{even}} \simeq \frac{2\pi}{u_{\min}^{\text{even}}} \simeq 65^\circ, \quad \theta_{\text{odd}} \simeq \frac{2\pi}{u_{\min}^{\text{odd}}} \simeq 130^\circ. \quad (22)$$

defining three different angular regions along the  $0^\circ - 180^\circ$  range where the  $C(\theta)$  function exhibits a different behaviour, as can be easily appreciated in Figures 1 and 3.

Now, from our discussion in the previous section on the Fourier expansion of the two-point angular correlation function, we will take into account that the  $C_{\text{even}}(\theta)$  and  $C_{\text{odd}}(\theta)$  pieces of Eq.(9) are associated to terms of the type  $\cos^2[n\theta]$  and  $\cos^2[(n+1/2)\theta]$ , respectively, as shown in Eqs.(11). Therefore, the lower limits for even and odd multipoles in the integral of Eq.(10) can be related to the infrared cutoffs  $k_{\min}^{\text{even,odd}}$  ( $u_{\min}^{\text{even,odd}}$ ), respectively.

Moreover, from the fit to the *Planck* 2018 data shown in Figure 3, the ratio  $u_{\min}^{\text{even}}/u_{\min}^{\text{odd}}$  turns out to be quite close to 2. This so far phenomenological fact will be understood further by considering the periodicity and antiperiodicity conditions applied to the maximum correlation lengths:

$$\frac{u_{\min}^{\text{even}}}{u_{\min}^{\text{odd}}} = \frac{k_{\min}^{\text{even}}}{k_{\min}^{\text{odd}}} = \frac{\lambda_{\max}^{\text{odd}}}{\lambda_{\max}^{\text{even}}} = 2, \quad (23)$$

as implied by Eq.(20). In the framework of the  $R_h = ct$  universe, this relation corresponds to two different exit times of the Planck regime: first the  $k_{\min}^{\text{odd}}$  mode and later the  $k_{\min}^{\text{even}}$  mode. In an inflationary scenario, it implies again two different times in a similar order but exiting the Hubble horizon. Needless to say, the above ratio 2 is expected to be valid only approximately, but we have exactly fixed it to this value in our numerical analysis.



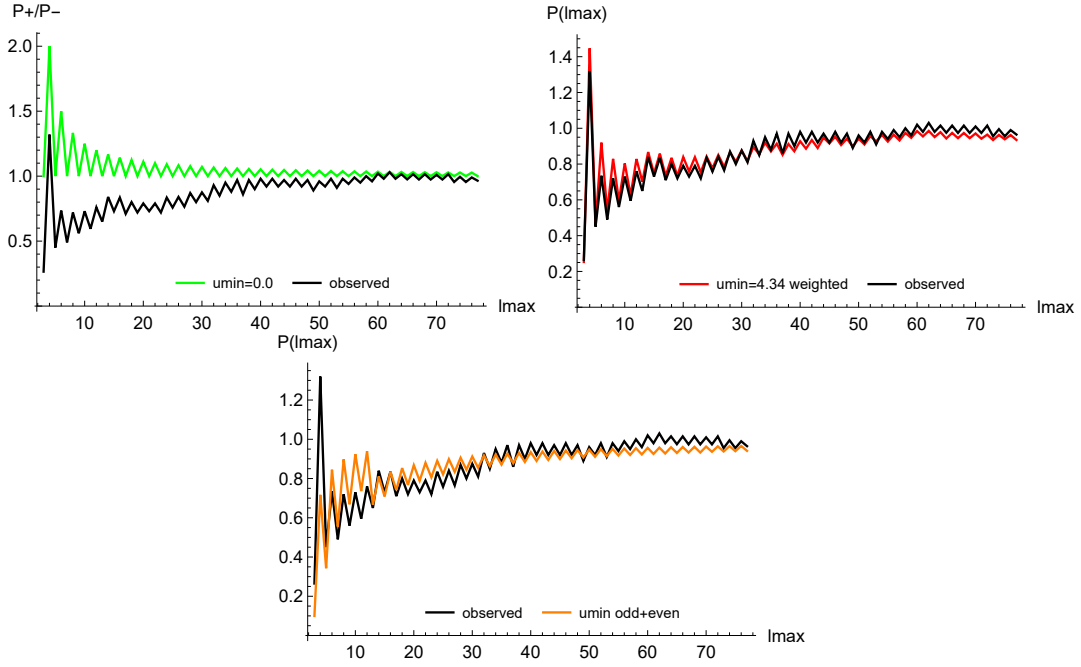


Figure 4:  $P(\ell_{\max})$  statistic as a function of  $\ell_{\max}$  compared to the *Planck* 2018 data for (a) Upper left panel:  $u_{\min} = 0$  and even-odd parity balance ( $\Lambda$ CDM). (b) Upper right panel:  $u_{\min} = 4.5$  and weighted  $C_\ell$  to get odd-parity dominance ( $\chi^2/\text{d.o.f.} \approx 1$ ). (c) Lower panel:  $u_{\min}^{\text{even}} = 5.34$  and  $u_{\min}^{\text{odd}} = 2.67$  ( $\chi^2/\text{d.o.f.} \approx 2$ ).

### 3.1 Parity statistic study

let us now address the deviation from the even-odd parity balance employing the parity statistic [21] as done in [12]

$$P(\ell_{\max}) = \frac{P^+(\ell_{\max})}{P^-(\ell_{\max})} ; \quad P^\pm(\ell_{\max}) = \sum_{\ell=2}^{\ell_{\max}} \gamma_\ell^\pm \frac{\ell(\ell+1)}{2\pi} C_\ell, \quad (24)$$

with the projectors defined as  $\gamma_\ell^+ = \cos^2(\ell\pi/2)$  and  $\gamma_\ell^- = \sin^2(\ell\pi/2)$ . Assuming that  $\ell(\ell+1) C_\ell \sim \text{constant}$  is satisfied at low  $\ell$ ,  $P^\pm$  can clearly be considered as a measurement of the degree of parity asymmetry. Any deviation from unity of this statistic points to an even-odd parity imbalance: below unity, it implies odd-parity dominance and vice versa. Below we apply this statistic to compare different fits with one or two infrared cutoffs.

In Figure 4 we plot  $P(\ell_{\max})$  as a function of  $\ell_{\max}$  corresponding to (a) upper left panel:  $u_{\min} = 0$  ( $\Lambda$ CDM); (b) upper right panel: our previous result for  $u_{\min} = 4.5$  and odd-parity dominance [12]; (c) lower panel: the new analysis performed in this paper assuming  $u_{\min}^{\text{even}} = 2u_{\min}^{\text{odd}} \simeq 5.34$ . As an aside, notice that the mean value of both  $u_{\min}^{\text{even,odd}}$  remains within the previous interval  $u_{\min} = 4.5 \pm 0.5$ . From inspection of these plots it becomes apparent that the fit using  $k_{\min}^{\text{odd,even}}$  pair somewhat worsens with respect to the single  $k_{\min} \neq 0$  case: the reduced  $\chi^2/\text{d.o.f.}$  increases from almost unity to about twice. Nonetheless, as already emphasized, the main interest of providing a common explanation to both missing large-angle correlations and odd-dominance, remains.

## 4 Discussion and conclusions

As claimed in Ref. [13], the lack of large-angle correlations observed in the CMB angular distribution from WMAP and *Planck* 2018 data can be accounted for by introducing an infrared cutoff  $k_{\min}$  to the CMB power spectrum, thereby implying a lower cutoff  $u_{\min}$  in the computation of all (odd and even) coefficients  $C_\ell$  of the multipole expansion in Eq.(2). Furthermore, the apparent odd-parity dominance manifesting as a downward tail at large angles ( $\theta \gtrsim 150^\circ$ ) can also be accommodated in the  $C(\theta)$  plot thanks to some extra weights mainly affecting the low-multipole coefficients  $C_\ell$ , ( $\ell \lesssim 10$ ), leading at the same time to an excellent fit of the parity statistics  $P(\ell_{\max})$  [12].

No obvious theoretical connection between such an infrared cutoff  $k_{\min}$  (i.e., lack of large-angle correlations) and parity imbalance has been found so far to our knowledge, but stressed their phenomenological compatibility [12], [25], [26]. In this paper, however, we have put forward a possible relationship between both anomalies by introducing to the CMB power spectrum two infrared cutoffs  $k_{\min}^{\text{even}}$  and  $k_{\min}^{\text{odd}}$ , whose ratio turns out to be close to 2 from a fit to the *Planck* 2018 dataset. In this way, we are able: (i) to reduce the number of fitting parameters with respect to [12], while reproducing the downward tail at large angles in the fit; (ii) to provide a theoretical connection (without actually resorting to any particular model) between both observations, setting the ratio  $k_{\min}^{\text{even}}/k_{\min}^{\text{odd}}$  exactly equal to 2.

Thus, new fits of  $C(\theta)$  and the parity statistic  $P(\ell_{\max})$  have been performed using the same *Planck* 2018 dataset, for the double infrared cutoff case. Since the number of fitting parameters is now considerably smaller than in [12], the goodness of the fits (determined by their  $\chi^2/\text{d.o.f.}$ ) somewhat worsens. However, let us emphasize the added value of our approach due to a common and suggestive explanation of both anomalies: missing correlations above  $\approx 70^\circ$  and a downward tail at  $\gtrsim 150^\circ$ .

On the basis of a Fourier analysis using a toy-model, we have associated even and odd multipoles of  $C(\theta)$  to periodic and antiperiodic boundary conditions satisfied by underlying (fermionic) fields of a composite inflaton, or a fermionic inflaton itself. Thus, the choice for the ratio  $k_{\min}^{\text{even}}/k_{\min}^{\text{odd}} = 2$ , becomes supported by theoretical arguments based on spin, beyond the initial heuristic approach, while the fits remain statistically acceptable.

As is well-known, spin degrees of freedom play a crucial role in elementary particle physics, e.g., predicting the gyromagnetic ratio  $g$  for the self-spinning electron to be about two times bigger than the value for an orbiting electron [27]. Needless to say, the famous muon  $g - 2$  deviation from zero stands as an important test of new physics, currently under close scrutiny [28]. The idea of searching for new physics and phenomena either at particle colliders and/or looking at the sky, in a complementary way, is certainly not new, being dark matter a good example of it.

Of course, explanations alternative to ours for missing large-angle correlations together with odd-parity dominance are possible: a statistical fluke of data at large angles, contamination effects, cosmic variance, or other underlying theoretical reasons.

Finally, let us point out that future very-high precision measurements of CMB polarization [29], [30], [31], might follow (or not) an angular pattern similar to the temperature fluctuations seen in the sky, thereby shedding light on this tantalizing hypothesis.

## Acknowledgments

I acknowledge inspiring discussions with V.Sanz at the beginning of this work. This work was partially funded by Spanish Agencia Estatal de Investigación under grant PID2020-113334GB-I00 / AEI / 10.13039/501100011033, and by Generalitat Valenciana under grant PROMETEO/2019/113 (EXPEDITE).

## References

- [1] Kolb, E.W.; Turner, M. *The early universe, Frontiers in Physics*, Westview Press 1994.
- [2] Di Valentino, E. et al. In the Realm of the Hubble tension: a Review of Solutions, *Class. Quantum Grav.* **2021** 38, 153001.
- [3] Brandenberger, R.H. Alternatives to the inflationary paradigm of structure formation, *Int. J. Mod. Phys. Conf. Ser.* 01 **2011**, 01, 67-79 [arXiv:0902.4731 [hep-th]].
- [4] Samart, D.; Pongkitivanichkul, C.; Channuie, P. Composite dynamics and cosmology: inflation, *Eur. Phys. J. Spec. Top.* **2022** <https://doi.org/10.1140/epjs/s11734-022-00446-4>.
- [5] Nambu, Y.; Jona-Lasinio, G. Dynamical Model of Elementary Particles Based on an Analogy with Superconductivity. *G., Phys. Rev.* **1961** 122, 345.
- [6] Gross, D.J.; Neveu, A. Dynamical symmetry breaking in asymptotically free field theories, *Phys. Rev. D* **1974**, 10, 3235.
- [7] Gunion, J.F.; Haber, H.E.; Kane, G.L; Dawson, S. *The Higgs Hunter's Guide*, *Front. Phys.* **80** (2000), pp. 339-349.
- [8] Melia, F. *The Cosmic Spacetime*, CRC Press, 2020.
- [9] Melia, F. A resolution of the Trans-Planckian problem in the  $R_h = ct$  universe, *PLB* **2021**, 818, 136632.
- [10] Perivolaropoulos, L. ; Skara, F. **2021**, unpublished, arXiv:2105.05208.
- [11] Vagnozzi, S.; Loeb, A. ; Moresco, M. Eppure e piatto? The cosmic chronometer take on spatial curvature and cosmic concordance, *Astrophys. J.* (**2021**) 908, 84.
- [12] Sanchis-Lozano, M.A.; Melia, F.; Lopez-Corredoira, M.; Sanchis-Gual, N. Missing large-angle correlations versus odd-dominance in the cosmic microwave background, *A&A* **2022** 10, 142-149. arXiv:2202.10987 [astro-ph.CO].
- [13] Melia, F.; López-Corredoira, M. Evidence of a truncated spectrum in the angular correlation function of the cosmic microwave background, *A&A* **2018** 610, A87.
- [14] Zwiebach, B. *A First Course in String Theory*, Cambridge University Press, 2004; p.p. 262-268.
- [15] Mukhanov, V. F. *Physical Foundations of Cosmology* (Cambridge University Press, Cambridge), 2005.
- [16] Melia F. Angular Correlation of the CMB in the  $R_h = ct$  Universe, *A&A* **2012** 561, A80.
- [17] Planck Collaboration, Aghanim, N. et al. Planck 2018 results. VI. Cosmological parameters, *A&A* **2018**, 641, A86.
- [18] Melia, F. Proper Size of the Visible Universe in FRW Metrics with Constant Spacetime Curvature, *Class. Quant. Grav.* **2013** 30, 155007.
- [19] Melia, F. Quantum Fluctuations at the Planck Scale, *EPJ-C* **2019** 79, 455.
- [20] Liu J., Melia F. Viability of slow-roll inflation in light of the non-zero  $k_{min}$  measured in the cosmic microwave background power spectrum, *Proc. R. Soc. A* **2020**, 476, 20200364.

- [21] Panda, S.; Aluri, P. K.; Samal, P. K.; Rath, P. K. Parity in Planck full-mission CMB temperature maps, *Astropart. Phys.* **2021** 125, 102493.
- [22] Abramowitz, M; Stegun, I. *Handbook of Mathematical Functions: with Formulas, Graphs, and Mathematical Tables*, Dover Books on Mathematics, 1970
- [23] Grams, G.; de Souza, R.; and Kremer, G. Fermion field as inflaton, dark energy and dark matter, *Class. Quant. Grav.* **2014** 31, 185008.
- [24] Copi, C.J. et al. Exploring suppressed long-distance correlations as the cause of suppressed large-angle correlations, *MNRAS* **2018** 000, 1-8.
- [25] Kim, J.; Naselsky, P.; Hansen, M. Symmetry and Antisymmetry of the CMB Anisotropy Pattern, *Adv. Astron.* **2012**, 960509.
- [26] Schwarz, D. J.; Copi, C. J.; Huterer, D.; Starkman, G. D. CMB anomalies after Planck, *CQG*, **2016** 33, 184001.
- [27] Thomson, M. *Modern Particle Physics*, Cambridge University Press, 2013; p.517.
- [28] P.A. Zyla et al. (Particle Data Group), *Prog. Theor. Exp. Phys.* **2020**, 083C01.
- [29] Bouchet, F. R. et al., COre (Cosmic Origins Explorer) A White Paper, **2011**, arXiv:1102.2181.
- [30] Hanany, S. et al. [NASA PICO] PICO: Probe of Inflation and Cosmic Origins, **2019**, arXiv:1902.10541.
- [31] Errard, J.; Feeney, S. M. et al. Robust forecasts on fundamental physics from the foreground-obscured, gravitationally-lensed CMB polarization, *JCAP I* **2016**, issue 03, article id. 052.